

# Augmentation of Fatigue and Tensile Strength of AA-6061 Processed through Equal Channel Angular Pressing

NAZEER AHMED ANJUM\*, SHAHID MEHMOOD\*, WAQAS ANWAR\*\*, ZAHID SULMAN\*, AND SAEED BADSHA\*\*\*

RECEIVED ON 24.02.2018 ACCEPTED ON 25.05.2018

## ABSTRACT

ECAP (Equal Channel Angular Pressing) is a technique used to enhance the strength of material by grain refinement. In this research, an aerospace grade aluminum alloy-6061 is investigated. The specimens were pressed through ECAP die channels, intersecting each other at an angle of  $90^\circ$  where a shear plane of  $45^\circ$  was developed, that results grains refinement. Fatigue strengths and CGR (Crack Growth Rate) for the stress ratio R 0.7 and 0.1 are found and compared with the as-received material. It was observed that the CGR is slower at stress ratio  $R=0.1$ , as compared to stress ratio  $R=0.7$ . An electric furnace was embedded with ECAP die to regulate the material flow through this die. The temperature of the die was maintained at  $450^\circ\text{C}$  during ECAP pressing and the specimens were also preheated at this temperature using another furnace. The ECAP die consists of two channels intersecting at  $90^\circ$  provided with safe inner and outer corner radius to avoid scaling. The microstructural observations revealed that the deformation was perfectly plastic. The ECAPed and as-received materials were also characterized by tensile tests, micro-hardness tests, and 3-point bend fatigue tests.

**Key Words:** Aluminium Alloy 6061, Equal Channel Angular Pressing, Crack Growth Rate, Fatigue, Paris Curve.

## 1. INTRODUCTION

Grain size is considered as a key microstructural factor affecting the mechanical and physical behavior of polycrystalline metals. Grain size is having a unique role to develop materials with desired mechanical properties. As the competition for better materials performance is never final, efforts to improve viable techniques for microstructure refinement, are continued. A promising boulevard for microstructure improvement of

metals is the use of SPD (Severe Plastic Deformation). There are many metal strengthening techniques used by the researchers since the material development history. Some of them are conventional (forging, rolling, extrusion etc.), it is obvious that these conventional techniques do not play an important role for grain refinement and hence strength increased up to a certain limit. To overcome this problem, some advanced techniques known as SPD techniques such as HPT

Authors E-Mail: (nazeer.anjum@uettaxila.edu.pk, shahid.mehmood@uettaxila.edu.pk, waqasanwar\_16@yahoo.com, zahid.suleman@uettaxila.edu.pk, saeed.badshah@iiu.edu.pk)

\* Department of Mechanical Engineering, University of Engineering & Technology, Taxila, Pakistan.

\*\* National Engineering and Scientific Commission of Pakistan.

\*\*\* International Islamic University, New Campus, Islamabad, Pakistan.

(High Pressure Torsion) [1], DCAP (Dissimilar Channel Angular Pressing) [2], ARB (Accumulative Roll Bonding) [3], ECAP [4] etc. were introduced. ECAP is typically used to strengthen light aluminum alloys through grain refinement [5-7]. ECAP method was introduced by Segal in the early 1980s. The material deformation of the material in ECAP is influenced by the non-linearity of the metals, temperature, mold geometry, ram speed, friction between specimen and die, and plunger shape [8-10]. The FCGR (Fatigue Crack Growth Rate) was also investigated for as-received and ECAPed specimens. FCGR is extension in the crack length per unit cycle, (da/dN) and is determined by slope of the FCG curve in Stage-II Region. Collini et. al. showed that specimens prepared from ECAP material had higher fatigue resistance compared to the base material [11-14].

## 2. EXPERIMENTAL SET UP

There are two channels in ECAP die, explicitly outlet and inlet channel as shown in Fig. 1. At the intersection of these passages two channels are formed. The inside angle is die angle ( $\phi$ ) and the outside angle is corner angle ( $\Psi$ ). The ECAP die and plunger were manufactured using tool steel AISI H13.

A hole was machined near the top edge of the plunger that provides connection with press ram using a bolt. The ECAP die was designed by considering the parameter: (i) shape of specimen, (ii) maximum pressing load, (iii) working temperature of specimen, (iv) size of specimen, (v) the die temperature.

At intersecting channels of die, corner radius of 8.45 mm, inner fillet radius of 3 mm was provided by preserving corner angle ( $\Psi$ ) of 22 degree. These angles avoid scaling of the billet. To heat the specimen along with die, a temperature controlled furnace shown in Fig. 1, which was fabricated on

the bed of hydraulic press for a smooth flow of material through ECAP die. The die and specimen was heated up to 450°C for a period of two hours. AHTIW (High Temperature Insulation Wool) was used for safety measurements to avoid heat dissipation. The die temperature was controlled by a control unit fitted with 4x950W heating elements. The overall capacity of hydraulic press was 100 tons.

The specimens for ECAP were prepared from as received material AA-6061, a plate with 22 mm thickness and specimens were prepared from this plate with dimension 20x20x120 mm<sup>3</sup>.

The mechanical properties of the tested material are shown in Table 1.

Before pressing these samples in ECAP die, the composition of the material was determined by XRF (X-Ray Fluorescence) and is given in Table 2.

The ECAP specimens were pressed through ECAP die channels at a constant ram velocity of 9 mm/sec. Before inserting the ECAP billet into the ECAP die inlet channel, a thin layer of Molykote graphite assembly grease was applied to overcome sticky behavior between billets and die channels. The die along with ECAP billet was heated up at 450°C for a smooth flow. Total twenty billets were pressed in the same environment and under same conditions. Then different specimens were prepared from the processes billet according to ASTM standards (E8, E64) for tensile testing, 3-point bend fatigue testing, microhardness testing, and metallography and fractographic analysis.

TABLE 1. MECHANICAL PROPERTIES OF AA-6061[2]

E (GPa)	$\sigma_u$ (MPa)	$\sigma_y$ (MPa)	Poisson's Ratio
70	310	270	0.33

TABLE 2. CHEMICAL COMPOSITION OF THE AL-6061 ALLOY

El	Mg	Fe	Si	Cu	Mn	V	Ti	Al
Wt%	1.08	0.17	0.63	0.32	0.15	0.01	0.02	Bal

The dog-bone shaped specimens were prepared by milling machining from as-received and ECAPed material according to ASTM-E8 standard [15].

The yield strength, ultimate tensile strength and percentage elongation were determined by applying unilateral load on MTS (Material Testing System). The machine has the capacity of 100 kN with different frequencies ranged from 1-60 Hz.

On the same machine, the fatigue tests were performed. Maximum load 1.25 kN and frequency 10 Hz were selected to perform 3-point bend fatigue tests. The experiments were performed for two different stress ratios ( $R = 0.1$  and  $0.7$ ) to

investigate the effect of CGR. Single edge notched specimens, as shown in Fig. 2, were prepared according to ASTM standard E647 on EDM (Electric Discharge Machine).

A clip-on-gauge was installed on notch to determine CMOD (Crack Mouth Opening Displacement) during fatigue testing. Using the values of CMOD, stress intensity was found. The obtained results were evaluated and crack ratio ( $a/w$ ) for every crack length was determined. The plots of CMOD and FCGR were plotted. The 3-point bend fatigue set-up is shown in Fig. 3, in which the specimen is supported at two roller supports and load is applied with the third roller at the midpoint of specimen. The clip on gauge is fixed to measure crack growth rate

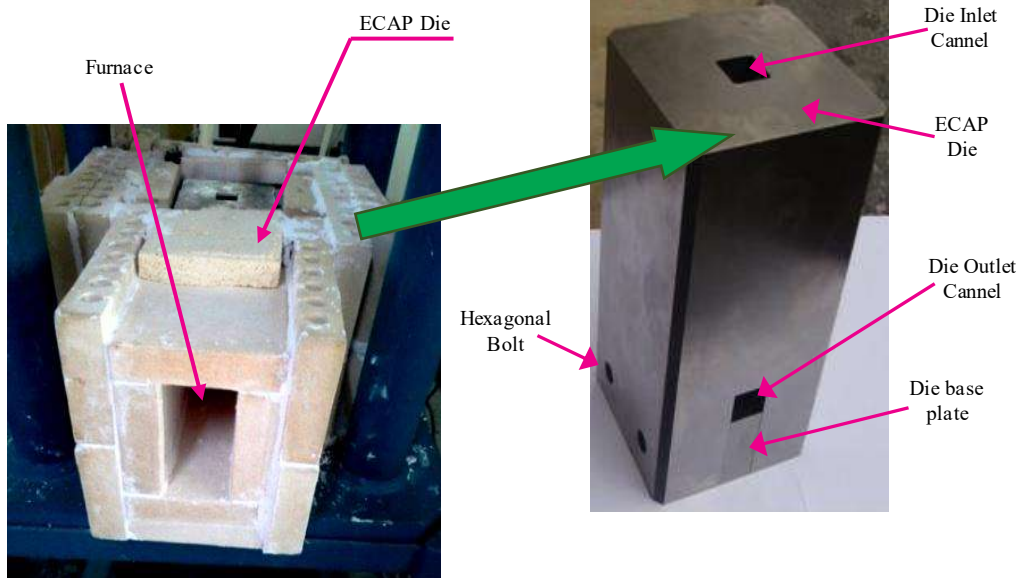


FIG. 1. ELECTRIC FURNACE (LEFT) AND ECAP DIE (RIGHT)

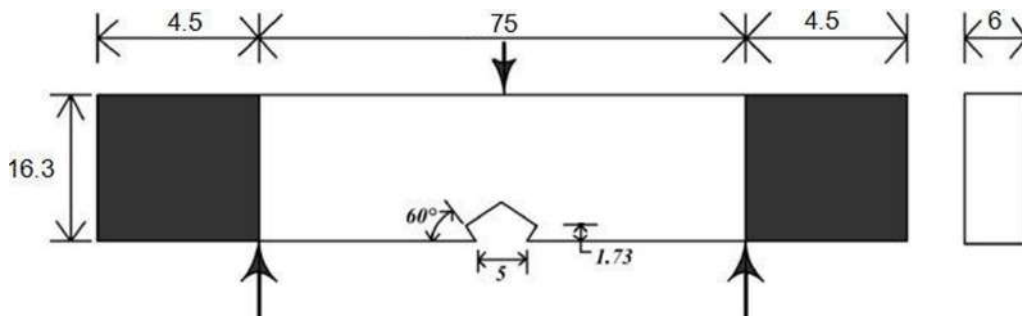


FIG. 2. 3-POINT BEND FATIGUE SPECIMEN (DIMENSIONS IN mm)

Rockwell and microhardness tests were performed to measure hardness before and after ECAP. A mirror-like surface was achieved by polishing according to ASTM E384 standard and micro-hardness tests were carried out for the load of 100 gram across the length of specimens.

The initial advancement of the current investigation is shown by step wise understanding of the ECAP process, shown in Fig. 4. Fig. 4(a) shows the shape of specimen modeled in ABAQUS™ with circular meshing and right side Fig. 4(a)

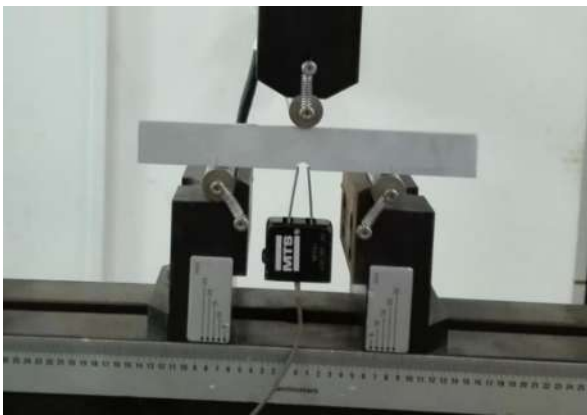


FIG. 3. 3-POINT BEND FATIGUE SPECIMEN

shows that circular rings is converted into an elliptical form. Fig. 4(b) is the specimen made from Teflon with circular slots filled with beads and its right side Fig. 4(b) shows that these circular rings is converted into an ellipse when processed through ECAP die. Fig. 4(c) shows the specimen made from the research material and its deformation is on its right side Fig. 4(c). The deformation of the grains was assessed by numerical simulation [12-14]. A circle was introduced in meshing and the arrangement of the circle after ECAP. This was confirmed using a billet of Nylon material. Then the experiments for AA 6061 carried out and specimens from the processed material were obtained for material characterization.

### 3. RESULTS AND DISCUSSION

The results of tensile test of as-received and ECAPed specimens are presented in Tables 3-4.

It is very clear that yield strength is increased by 14.0%, Rockwell hardness by 24% whereas tensile strength is increased by 34.4% of ECAPed specimens.

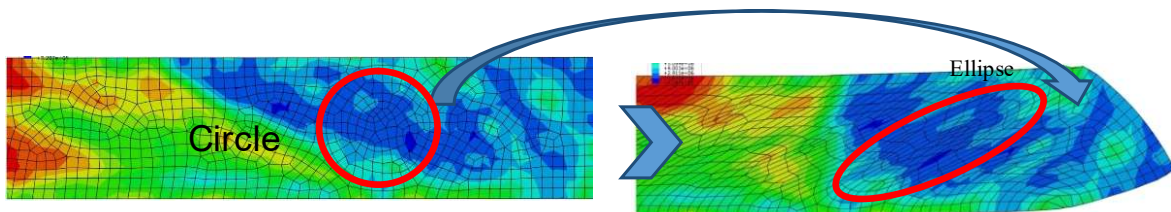


FIG. 4(a). SIMULATION



FIG. 4(b). EXPERIMENTAL VERIFICATION

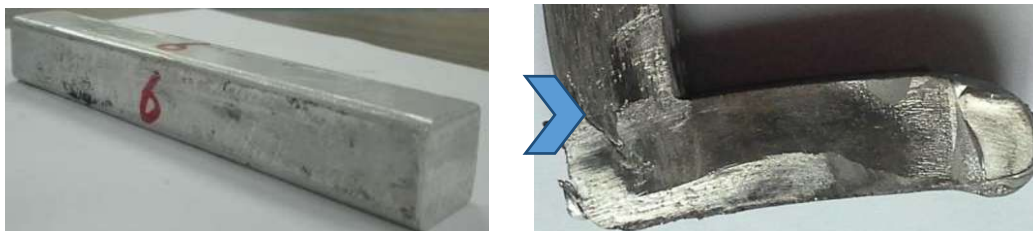


FIG. 4(c). REAL EQUAL CHANNEL PRESSING OF THE SPECIMEN

For fatigue analysis 3-point bend testing was adopted. The relation between stress intensity factor  $\Delta K$  for  $R=0.1$  and  $0.7$  are shown in Fig. 5.

Equation (1) is helpful to determine stress intensity factor  $\Delta K$ . The crack started early for smaller values of  $\Delta K$  for as-received whereas having higher magnitude for the material processed by ECAP. This is because the ECAP process has enhanced fracture toughness.

The fatigue crack length “a” was determined by installing a digital microscope on fatigue testing apparatus MTS. Equation (1) was used to determine crack ratio [16].

$$\frac{a}{W} = 0.9997 - 3.95U + 2.982U^2 - 3.214U^3 + 51.52U^4 - 113.0U^5 \quad (1)$$

TABLE 3. TENSILE TEST RESULTS OF AL 6061

Specimen Type	$\sigma_y$ (MPa)	$\sigma_u$ (MPa)
Al 6061 as-received	270	320
Al 6061 ECAPed	310	430

TABLE 4. VICKERS HARDNESS FOR SINGLE PASS OF AL-6061

Specimen Type	Al-6061 as-received	Al-6061 ECAP
Hardness (HRC)	27	34

$$U = \frac{1}{\left\{ 1 + \sqrt{\left[ \left( \frac{E'BWm}{P} \right) \left( \frac{4W}{S} \right) \right]} \right\}} \quad (2)$$

Where  $\nu$  is Poisson’s Ratio,  $E'$  is Effective young’s modulus, and  $E'$  is  $E(1-\nu^2)$  for plane strain.

The stress intensity factor of 3-point bend test of 6061-T6 Aluminum alloy was determined by Equation (3) [17].

$$K = \left( \frac{PS}{BW^{\frac{3}{2}}} \right) * f\left( \frac{a}{W} \right) \quad (3)$$

$f(a/W)$  is the geometric correction factor which is given in Equation (4).

$$f\left( \frac{a}{w} \right) = \frac{3 \sqrt{\left( \frac{a}{w} \right) \left[ 1.99 - \left( \frac{a}{w} \right) \left( 1 - \frac{a}{w} \right) \left( 2.15 - 3.93 \left( \frac{a}{w} \right) + 2.7 \frac{a^2}{w^2} \right) \right]}}{2 \left( 1 + 2 \frac{a}{w} \right) \left( 1 - \frac{a}{w} \right)^{\frac{3}{2}}} \quad (4)$$

The Paris curves for both ECAP materials and as-received were drawn [18-19]. During fatigue crack propagation, crack length was assessed from the CMOD data obtained from MTS. This data was used to develop paris curves for

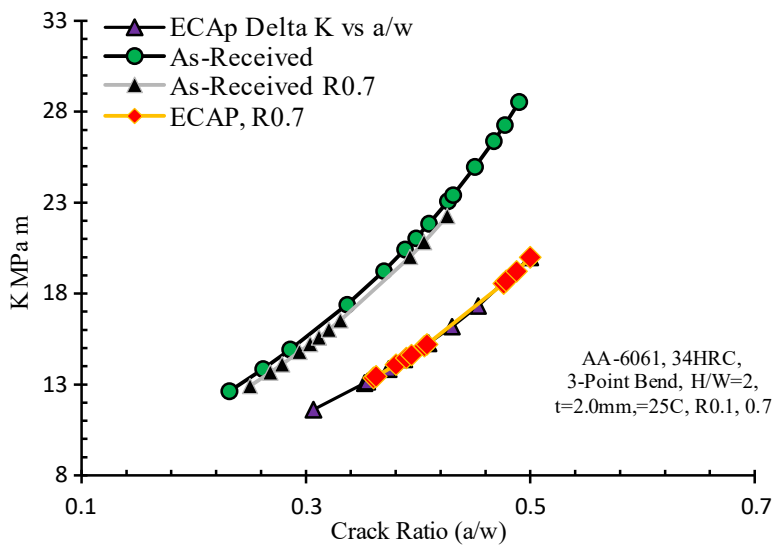


FIG. 5. RELATION BETWEEN CRACK RATIO AND K

ECAPed and as-received materials by considering two stress ratio,  $R=0.1$  and  $R=0.7$ , shown in Fig. 6. The crack growth is obviously slower in the ECAP samples compared to the as received material. This slow rate is mainly due to increased strength of the materials as processed by ECAP.

The values of  $\Delta K$  in section of  $19-28 \text{ MPa}\sqrt{\text{m}}$ , crack growth ( $da/dN$ ) are relatively stable at stress ratio  $R=0.1$ . For  $\Delta K > 28 \text{ MPa}\sqrt{\text{m}}$ , the CGR reveals a sudden acceleration in the as-received samples while ECAP specimen give sunlike behavior.  $\text{MPa}\sqrt{\text{m}}$ , an acceleration in CGR was seen for  $\Delta K \leq 31$  but for higher values of  $\Delta K$  CGR retards. The CGR in the ECAP samples is slower at the stress ratio  $R=0.7$  compared with the as-received material. This slow rate of CGR is due to augmented mechanical properties of the materials as processed by ECAP.  $\Delta K$  values in the section from  $20-28 \text{ MPa}\sqrt{\text{m}}$ , and CGR ( $da/dN$ ) is relatively stable at stress ratio  $R=0.7$ .

The  $\Delta K$  values are more than  $28 \text{ MPa}\sqrt{\text{m}}$ , and CGR shows a sudden acceleration in as-received sample while in ECAP specimens, an acceleration in CGR was seen up to  $28 \text{ MPa}\sqrt{\text{m}}$  of  $\Delta K$  but for higher values, it is slowdown. The results suggest that the higher values of  $\Delta K$  give less distributed

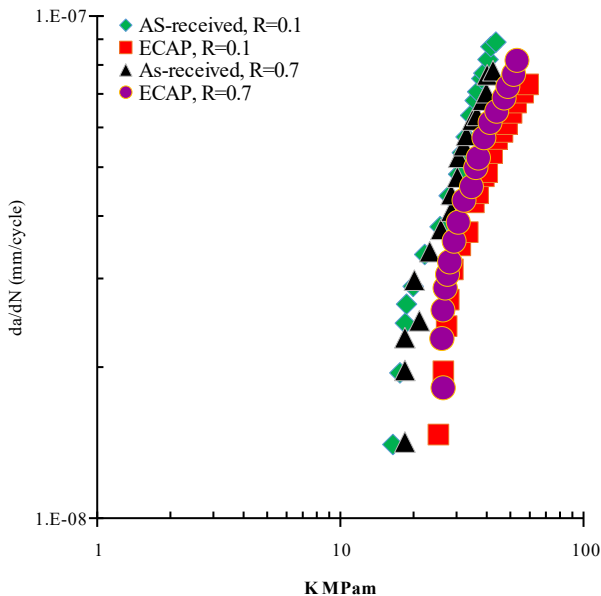


FIG. 6. LOG-LOG PLOT OF AS-RECEIVED AND ECAP SPECIMENS BETWEEN FATIGUE CRACK GROWTH RATE AND  $\Delta K$  AT STRESS RATIOS  $R=0.1$  AND  $R=0.7$

data points as compared to the smaller  $\Delta K$  values. This variance is because of the interaction between cyclic plastic zones and their consequence on fatigue damage. The CGR is abrupt in as-received material than the ECAPed samples. The association of crack length and crack ratio is presented in Fig. 7. The ASTM E399 standard cannot be pragmatic to estimate crack length by CMOD if large crack closure exists as this only allows up to a limited crack length [16]. At the stress ratio of  $R=0.1$ , the difference between the samples of as-received and ECAPed materials indicates that CMOD is more in later samples. This difference is due to the fine-tuning of the grains and therefore strengthening of the material. For the stress ratio  $R=0.7$  crack ratio ( $a/w$ ) of as-received material is smaller than the ECAPed material. The slope of the trend line of as-received is more than the ECAPed material which is although very close that of ECAPed material.

In Fig. 8, The behavior of CGR against  $\Delta K_{\text{max}}$  for as-received material and ECAPed samples is given. The curves show that the rift started at the estimated identical  $K_{\text{max}}$  for both. However, CGR of the ECAPed material is comparatively slower than that of as-received material, which manifests improvement in the toughness by ECAP.

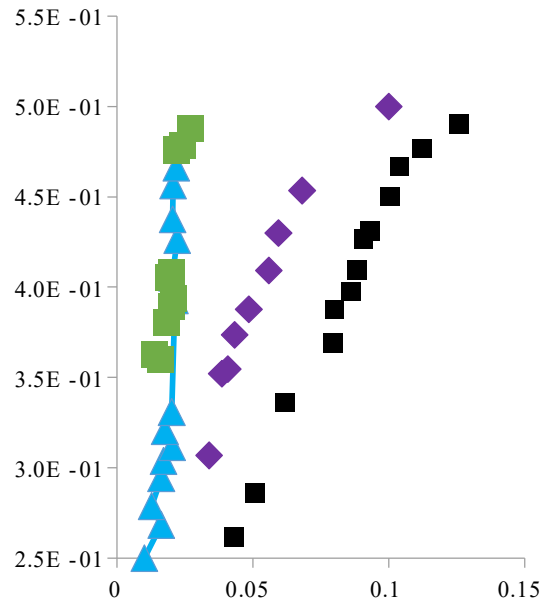


FIG. 7. COMPARISON BETWEEN CMOD AND CRACK RATIO ( $a/w$ ) AT  $R=0.1$  AND  $R=0.7$



The CGR is slower in ECAPed samples than the as-received material and is associated to the augmentation of material strength in terms of its hardness, toughness, yield strength, ultimate strength and fatigue strength by ECAP processing of the investigated material.

The appearance of the grain structure of the samples is given in Fig. 9. For as-received material the size of the grains is course whereas very fine for the ECAPed one. This was because of the plastics deformation of the material by ECAP pressing. Plastic deformation of the material by pure shear (45 degree) was observed by numerical simulation. Previous results of current work clearly prove the advantage of ECAP to enhance the material properties without any heat treatment, change in its composition and change in cross-sectional size.

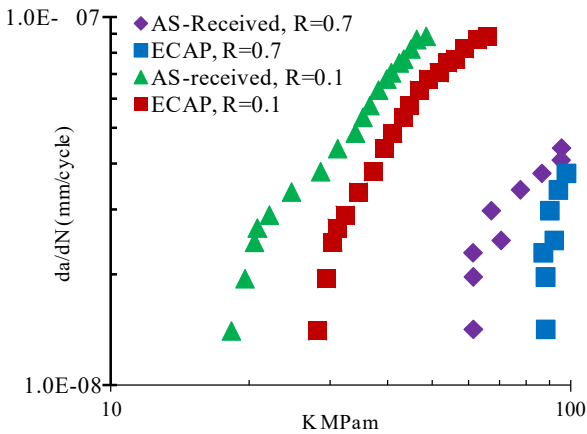
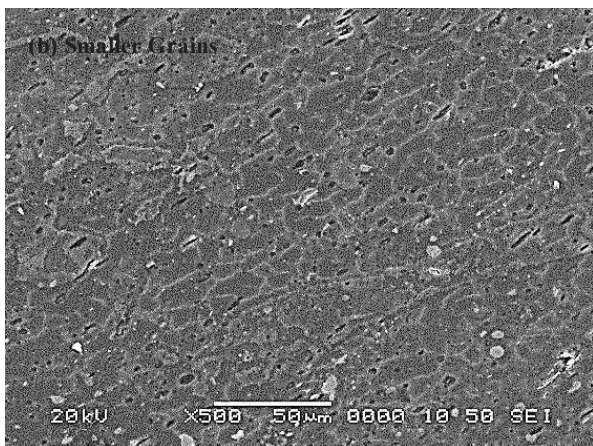


FIG. 8. LOG-LOG PLOT BETWEEN  $K_{MAX}$  AND FATIGUE CRACK GROWTH RATE ( $da/dN$ ) AT STRESS RATIOS,  $R=0.1$ , AND  $0.7$

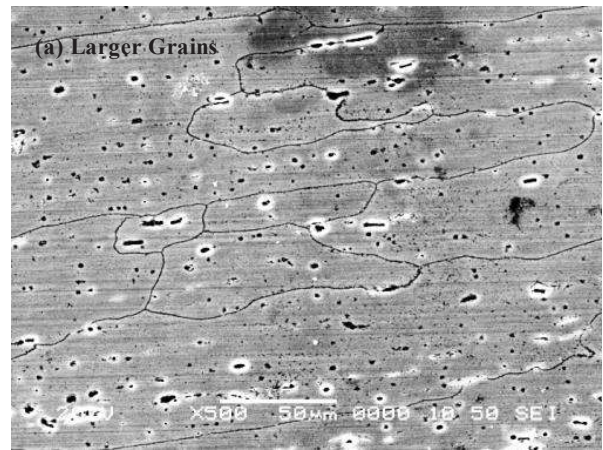


(a) AS-RECEIVED

#### 4. CONCLUSIONS

In this work, the ECAP of the aluminum alloy 6061 was carried out. The mechanical properties such as yield strength, ultimate tensile strength, micro hardness, CGR and fatigue strength were determined and compared with as-received material. Following are the main outcomes:

- (i) Firstly, the method of ECAP is conceptualized through simulation and processing of relatively softer material, in which, internal plasticity of the material can be visualized in a simple way.
- (ii) By ECAP processing of the aluminum alloy 6061, the yield strength is increased by 14%, hardness 24%, and ultimate tensile strength 34.37%.
- (iii) The improvement in the fatigue strength was also found ECAP process.
- (iv) Stress intensity of the investigated material after ECAP is measured with respect to CGR. It is found that stress intensity is quite low in the ECAPed material. Also the effect of stress ratio is found negligible.
- (v) Paris curve for the ECAPed and as-received material are determined for the stress ratios of 0.1 and 0.7. It is found that the CGR in the ECAPed material is low in ECAPed material for both stress ratios.
- (vi) SEM observations are clearly proving the grain size refinement by ECAP of Aluminum alloy 6061 in current study.



(b) ECAPED

FIG. 9. GRAIN APPEARANCE AT SCALE OF 500X

## ACKNOWLEDGEMENT

This research work was supported and funded by University of Engineering & Technology, Taxila, Pakistan, under Research Grant No. FME-ME149. Special appreciations to Institute of Space Technology, to provide facilities of SEM and technical support to accomplish this research work.

## REFERENCES

- [1] Jiang, H., Zhu, Y.T., Butt, D.P., Alexandrov, I.V., and Lowe, T.C., "Microstructural Evolution, Microhardness and Thermal Stability of HPT-Processed Cu", *Materials Science & Engineering-A*, Volume 290, pp. 128-138, 2000.
- [2] Tan, E.A., Kibar, A., and Gür, C.H., "Mechanical and Microstructural Characterization of 6061 Aluminum Alloy Strips Severely Deformed by Dissimilar Channel Angular Pressing", *Materials Characterization*, Volume 62, pp. 391-397, 2011.
- [3] Su, L., Lu, C., Tieu, A.K., Deng, G., and Sun, X., "Ultrafine Grained AA1050/AA6061 Composite Produced by Accumulative Roll Bonding", *Materials Science and Engineering-A*, Volume 559, pp. 345-351, 2013.
- [4] Zhao, Y., Guo, H., Shi, Z., Yao, Z., and Zhang, Y., "Microstructure Evolution of TA15 Titanium Alloy Subjected to Equal Channel Angular Pressing and Subsequent Annealing at Various Temperatures", *Journal of Materials Processing Technology*, Volume 211, pp. 1364-1371, 2011.
- [5] Iwahashi, Y., Horita, Z., Nemoto, M., and Langdon, T.G., "An Investigation of Microstructural Evolution during Equal-Channel Angular Pressing", *Acta Materialia*, Volume 45, pp. 4733-4741, 1997.
- [6] Segal, V., "Equal Channel Angular Extrusion: From Macromechanics to Structure Formation", *Materials Science and Engineering-A*, Volume 271, pp. 322-333, 1999.
- [7] Zhu, Y.T., and Low, T.C.E., "Observations and Issues on Mechanisms of Grain Refinement during ECAP Process", *Materials Science and Engineering-A*, Volume 291, pp. 46-53, 2000.
- [8] Jin, Y.G., Baek, H.M., Im, Y.-T., and Jeon, B.C., "Continuous ECAP Process Design for Manufacturing a Microstructure-Refined Bolt", *Materials Science and Engineering-A*, Volume 530, pp. 462-468, 2011.
- [9] Chen, D.C., and Chen, C.P., "Investigation Into Equal Channel Angular Extrusion Process of Billet with Internal Defects", *Journal of Materials Processing Technology*, Volume 204, pp. 419-424, 2008.
- [10] Ma, K., Wen, H., Hu, T., Topping, T.D., Isheim, D., and Seidman, D.N., "Mechanical Behavior and Strengthening Mechanisms in Ultrafine Grain Precipitation-Strengthened Aluminum Alloy", *Acta Materialia*, Volume 62, pp. 141-155, 2014.
- [11] Valiev, R.Z., Murashkin, M.Y., Bobruk, E.V., and Raa, G.I.B., "Grain Refinement and Mechanical Behavior of the Al Alloy, Subjected to the New SPD Technique", *Materials Transactions*, Volume 50, pp. 87-91, 2009.
- [12] Rosochowski, A., and Olejnik, L., "Numerical and Physical Modelling of Plastic Deformation in 2-Turn Equal Channel Angular Extrusion", *Journal of Materials Processing Technology*, Volume 125, pp. 309-316, 2002.
- [13] Li, S., Bourke, M.A.M., Beyerlein, I.J., Alexander, D.J., and Clausen, B., "Finite Element Analysis of the Plastic Deformation Zone and Working Load in Equal Channel Angular Extrusion", *Materials Science and Engineering-A*, Volume 382, pp. 217-236, 2004.
- [14] Gilioli, A., Manes, A., and Giglio, M., "Numerical Simulation of a Fracture Toughness Test of an Al6061-T6 Aluminium Alloy Using a Ductile Criterion", *Mechanics Research Communications*, Volume 58, pp. 2-9, 2014.
- [15] Standard-A, "E8M-04," Standard Test Method for Tension Testing of Metallic Materials", Philadelphia, American Society for Testing and Materials, 2004.
- [16] Standard-A, "E399-90," Standard Test Method for Plane Strain Fracture Toughness of Metallic Materials", Philadelphia, American Society for Testing and Materials, 1993.
- [17] H.-S.L.-A. Steels, "Properties and Selection: Irons, Steels, and High-Performance Alloys", *ASM International Handbook*, Volume 1, pp. 389, 1990.
- [18] Dinda, S., and Kujawski, D., "Correlation and Prediction of Fatigue Crack Growth for Different R-Ratios Using K Max and DK+ Parameters", *Engineering Fracture Mechanics*, Volume 71, pp. 1779-1790, 2004.
- [19] Kujawski, D., "Enhanced Model of Partial Crack Closure for Correlation of R-Ratio Effects in Aluminum Alloys", *International Journal of Fatigue*, Volume 23, pp. 95-102, 2001.
- [20] Kujawski, D., "A New (AK+K Max) 0.5 Driving Force Parameter for Crack Growth in Aluminum Alloys", *International Journal of Fatigue*, Volume 23, pp. 733-740, 2001.
- [21] Kujawski, D., and Ellyin, F., "A Fatigue Crack Growth Model with Load Ratio Effects", *Engineering Fracture Mechanics*, Volume 28, pp. 367-378, 1987.